



LAWRENCE  
LIVERMORE  
NATIONAL  
LABORATORY

# Optimal Heat Collection Element Shapes for Parabolic Trough Concentrators

C.L. Bennett

November 16, 2007

Journal of Solar Energy Engineering

## **Disclaimer**

---

This document was prepared as an account of work sponsored by an agency of the United States government. Neither the United States government nor Lawrence Livermore National Security, LLC, nor any of their employees makes any warranty, expressed or implied, or assumes any legal liability or responsibility for the accuracy, completeness, or usefulness of any information, apparatus, product, or process disclosed, or represents that its use would not infringe privately owned rights. Reference herein to any specific commercial product, process, or service by trade name, trademark, manufacturer, or otherwise does not necessarily constitute or imply its endorsement, recommendation, or favoring by the United States government or Lawrence Livermore National Security, LLC. The views and opinions of authors expressed herein do not necessarily state or reflect those of the United States government or Lawrence Livermore National Security, LLC, and shall not be used for advertising or product endorsement purposes.

## **Optimal Heat Collection Element Shapes for Parabolic Trough Concentrators**

Charles L. Bennett

Lawrence Livermore National Laboratory, Livermore, CA 94550

For nearly 150 years, the cross section of the heat collection tubes used at the focus of parabolic trough solar concentrators has been circular. This type of tube is obviously simple and easily fabricated, but it is not optimal. It is shown in this article that the optimal shape, assuming a perfect parabolic figure for the concentrating mirror, is instead oblong, and is approximately given by a pair of facing parabolic segments.

### **Introduction**

In 1868, John Ericsson submitted a thesis on “The Use of Solar Heat as a Mechanical Motor-Power”, to the Swedish University in Lund [1], for which he was awarded an honorary Ph.D.. A drawing [2] of his parabolic trough, see Fig. 1, built in New York in 1883, shows a remarkable similarity to the state of the art solar concentrators today, and clearly displays a circular cylindrical heat collection element at the focus of the parabolic trough. Today, concentrating solar thermal power is on the verge of economic viability. The most widely deployed

solar thermal power plants currently are based on parabolic trough concentrating mirrors with central heat collection elements comprised of hollow receiver tubes that lie along the focal axis of the concentrating mirror. One of the important factors in the cost effectiveness of solar thermal power is the thermal efficiency of these heat collection elements. Heat loss from these elements, particularly for vacuum insulated tubes, is dominated by thermal radiation from the surface of the tube. In a recent systems analysis [3] the observed thermal efficiency for modern solar heat collection elements at the focus of parabolic trough concentrators near the time of an equinox is only 60% at a solar insolation of  $800 \text{ W/m}^2$  and actually drops to 55% at a peak solar insolation of  $1000 \text{ W/m}^2$ . These efficiency numbers include important contributions both from the orientation of the solar concentrator mirrors, and the size and shape of the heat collection elements. In the body of the text below, it is shown how the quantitative heat collection efficiency depends on the size and shape of the heat collection elements. It is found that greater heat collection efficiency may be obtained with an oblong heat collection element than with the conventional circular heat collection element.

## Early Studies

Prior studies on the “optimal” shapes for solar heat collectors assumed that the optimum shape is the minimal area shape still capable of intercepting all rays from the sun. For example, Ries and Spirkel [4] present a general recipe for the construction of such minimum surface absorbers, derived from the caustic curves associated with the edge rays produced by a given concentrator mirror shape. Following their recipe for an  $f/D=0.25$  concentrating mirror leads to the profile labeled “Caustic” in Fig. 2. In contrast, Cobble [5] found that the optimal absorber shape for a parabolic mirror having  $f/D=0.25$  was that of two facing parabolas. The profile labeled “Parabolas” in Fig. 2 represents this case. For comparison, a simple rhombus, having a height twice the width, is also displayed in Fig. 2.

In practice, there is a significant spread in the distribution of concentrated sunlight seen near the focal region, both because there is some spread produced as sunlight passes through the atmosphere, but more importantly, because economically practical solar concentrator mirrors have significant aberrations. For this reason, it is not necessarily true that the optimal absorber is the minimum area shape still capable of intercepting “all” rays from the sun. Rather, here the optimal absorber is defined as that shape that yields the maximum net solar heat collection, with the losses produced by the extent of the absorber surface area included. For this optimization, it is important to consider not only a reasonably accurate model for the reflected solar flux angular distribution seen near the

focus, but also to include a reasonably accurate model for the radiative losses from the surface of the heat collection elements themselves, in order to find a pragmatically optimal collector shape.

### **Solar Flux Angular Distribution**

The reflection of a representative distribution of solar rays incident at point A on the surface of a parabolic trough mirror is illustrated in Fig. 3 in terms of the projection onto the plane perpendicular to the longitudinal axis of the parabolic trough. Figure 3 also shows a schematic illustration of the qualitative transformation from the incoming solar flux distribution (dominated by the sun's radiance distribution and atmospheric scattering) to the outgoing reflected solar flux distribution (dominated by normally distributed mirror associated errors). The schematic illustration of the incoming solar flux angular distribution shown corresponds to the intensity across the width of the narrower incoming ray fan that converges onto point A. The schematic illustration of the reflected solar flux angular distribution corresponds to the intensity across the width of the wider outgoing ray fan that diverges from point A and is generally directed to the focus at point F in the figure.

The quality of parabolic trough concentrating mirrors used in modern solar thermal energy power plants is quite good, and with proper alignment, the width of the angular spread of reflected sunlight is substantially independent of location on the mirrors. For example, in work reported by Wendelin [6], mirror surface

r.m.s slope errors at the Solargenix Advanced Parabolic Trough Pilot Project were 4.4 mrad for the Starnet Space frame, and 3.0 mrad for the improved Gossamer Spaceframe. Even though these r.m.s. slope errors are numerically smaller than the angular diameter (8.5 mrad) of the sun, upon reflection, the resulting distribution of reflected intensity seen at the focus of a solar concentrator still tends to be dominated, not by the angular diameter of the sun, but by the r.m.s. mirror slope errors.

The impact of normally distributed mirror surface slope errors on the distribution of reflected sunlight near the line focus of a parabolic trough solar concentrator has been shown by Bendt et al. [7], to be determined by the following expression for the variance of the Gaussian distribution describing the projected and reflected rays.

$$\sigma^2 = 4\sigma_{\perp}^2 + 4\sin^2\frac{\beta}{2}\tan^2\theta_{\parallel}\sigma_{\parallel}^2 \quad (1)$$

The choice of coordinates used is indicated in Fig. 3. The x-y coordinate system is chosen to define the plane perpendicular to the longitudinal symmetry axis of the trough. The origin in the x-y plane is chosen to be at the center C of the trough. The angle  $\beta$  is that between the directions for the center of the reflected light distribution projected into the x-y plane and the y-axis. The elevation angle out of the x-y plane of the incident solar flux is given by  $\theta_{\parallel}$ . The variance of the mirror slope errors for variations within the x-y plane is given by  $\sigma_{\perp}^2$ , while the variance

of the mirror slope errors perpendicular to the x-y plane is given by  $\sigma_{\perp}^2$ . In the derivation of Eq. (1) it is assumed that the slope errors in the x-y plane are statistically independent of the slope errors in the perpendicular plane.

For the case that the aperture of the parabolic trough is perpendicular to the direction to the sun, so that  $\theta_{\parallel}$  vanishes, the variance of the slope errors perpendicular to the x-y plane makes no contribution to  $\sigma$ . Two axes of angular tracking are required in order to force  $\theta_{\parallel}$  to always vanish. However, for a single axis of angular tracking, with a polar mount, so that the rotation axis is parallel to the Earth's rotation axis,  $\theta_{\parallel}$  may be held to less than  $23.5^{\circ}$  in magnitude throughout the year. The extreme value of  $23.5^{\circ}$  is only reached during the summer and winter solstices. This angle is small enough that the angular spread of reflected solar rays is approximately independent of the location of the reflection point on the mirror and also approximately independent of time. This approximation is not valid for horizontally oriented troughs, however, and an accurate treatment for horizontal troughs must take into account the position dependent, and time dependent spread in the reflected sunlight.

### **Collection Efficiency vs. Collector Element Shape**

For a Gaussian intensity distribution, the fraction of the sunlight reflected from a given position on the mirror that strikes the central heat collection element is given by the following expression.

$$\text{Fraction hitting heat collection element} = \text{erf}\left(\frac{\omega}{\sigma\sqrt{8}}\right) . \quad (2)$$

In this expression,  $\omega$  is the angular width of the heat collection element, as seen from the point of reflection, and  $\sigma$  is given by the square root of Eq. (1). The angular width  $\omega$  depends not only on the point of reflection, but the size and shape of the heat collection element itself. For the case of a circular tube of diameter  $d$ , the angular width  $\omega$  depends on the distance  $r$  from the point of reflection to the focus given, to first order approximation in  $d/r$ , by the expression

$$\omega_{\text{circular\_tube}} \approx \frac{d}{r} . \quad (3)$$

Next consider the case of a rhombus, with height  $h$ , and width  $w$ , illustrated in Fig. 4. The following relation gives the approximate angular width  $\omega$  for this case, to first order approximation in  $w/r$  and  $h/r$ .

$$\omega_{\text{rhombus}} \approx \max\left(\frac{w \cos\beta}{r}, \frac{h \sin\beta}{r}\right) \quad (4)$$

The fraction of the incident sunlight at the aperture of the concentrator mirror that is absorbed by the collector depends on the nature of the surface of the heat collection element, including its roughness and composition, the local angle of incidence, the reflectivity of the concentrator mirror, and the wavelength of the incident light. For simplicity, it will be assumed here that the fractional reflectivity times absorption is a fixed constant,  $\alpha$ , that is independent of the angle of incidence and wavelength of light. This is a reasonable approximation for

many combinations of black absorbers and shiny reflectors. In this case, the fractional solar intensity absorbed differs from Eq. (2) only by the factor  $\alpha$ :

$$\text{Fractional absorption} = \alpha \cdot \operatorname{erf}\left(\frac{\omega}{\sigma\sqrt{8}}\right). \quad (5)$$

The net thermal power produced by the heat collection element is given by integrating the power absorbed for light incident over the full range of horizontal positions across the width  $D$  of the concentrator mirror aperture and subtracting the thermal power re-radiated by the heat collection element itself. In the present work, both the integration of the absorbed light over the range of incident angles, and the integration of re-radiated power by the heat collection element over the range of emission angles were performed numerically. In view of the complexity of the various shapes considered, especially that labeled “Caustic” in Fig. 2, and discussed later, it is quite difficult to represent these results as closed form analytic expressions.

A number of examples of the net power so produced are shown in Fig. 5 as a function of the width of the rhombus (relative to the parabolic mirror focal length) for various values of the ratio of the focal length  $f$  to the aperture diameter  $D$ . Corresponding examples of the net power for a circular tube are shown in Fig. 6. The specific assumptions used in both of these cases are listed in table 1, and represent approximately the conditions found in currently deployed parabolic trough solar thermal power plants.

**Table 1. Heat collection system parameters**

Parameter	Value
Heat Collector Surface Temperature	700 K
Thermal Emissivity of Heat Collector Surface	0.19
Mirror Reflectivity * Collector Absorbance	90%
Direct Normal Incident Flux	800 W/m <sup>2</sup>
r.m.s. Width of Reflected Sunlight	5.5 mrad

The reason for the nearly linear falloff in net power collection for larger size collection elements is that as the angular width becomes more than about three or four times the width of the reflected sunlight distribution, the error function values (cf. Eq. 5) approach unity while the re-radiation losses continue to grow linearly with the dimensions of the heat collection element. The value of the diameter to focal length ratio for the LS-3 heat collection elements used in the SEGS plants is indicated by the arrow in Fig. 6, and it can be seen that this is very close to the optimal circular tube diameter.

The maximum net power for the rhombic collector occurs for the ratio  $f/D=0.17$  while the maximum net power for the circular tube collector occurs for the ratio  $f/D=0.20$  for the parameters listed in table 1. The value of the rhombus height to width ratio that yielded the global maximum net power was 2.12, but the maximum net power is fairly insensitive to this ratio. The variation in net

collected power for the rhombic collector is compared with the circular collector in Fig. 7 as a function of collector size. It is found that there is a net power advantage of approximately 2.5%, for the rhombic shape at its optimal size compared to the circular tube at its optimal size.

The other two heat collection element profiles previously discussed in the literature, labeled in Fig. 2 as “Parabolas” and “Caustic”, were analyzed in a similar fashion as for the rhombus and circle. Figure 8 shows the fractional absorption (without including thermal losses) as a function of the mean width to focal length ratio for each of the profiles. In each case, the mean width is defined as the angle averaged projected width of each profile. It is this mean width that determines the radiative heat loss from the surface of the profile. Also, for this analysis, the  $f/D$  for the parabolic concentrating mirror was taken to be 0.25 for all cases. It can be seen that the fractional absorption is nearly identical for each of the three cases: “Caustic”, “Rhombus” and “Parabolas”, and all three have significantly more absorption, for a given radiative heat loss, than the circular tube. The basic reason for the very similar behavior for all of the various profiles considered is that the smearing out of the reflected sunlight distribution inherently damps out sensitivity to the fine details of the collector element shape.

In order to examine the quantitative impact that the Gaussian smearing has in this analysis, the fractional absorption for the same four profiles was calculated for the case of a perfect parabolic mirror and no atmospheric scattering. These

results are displayed in Fig. 9. In this case, there is a more significant dependence on the shape of the collector profile. Whether or not Gaussian smearing was included, the profile corresponding to facing parabolic segments proved to have the highest performance. Although this analysis does not rigorously prove that the facing parabolic segments profile is the mathematically optimum shape, in view of the insensitivity to the fine details, as seen by the small differences between all three oblong shapes with a realistic degree of Gaussian smearing, it is clearly pragmatically optimal, and it is also clear that only a moderate degree of engineering tolerance is required for the manufacture of this component.

### **Conclusions**

From the results of the calculations displayed in this work, it can be seen that the circular cross section solar heat collection element is not optimal in terms of the efficiency for the collection of solar energy. Among the profiles considered, the highest collection efficiency was found for a shape corresponding to a pair of parabolic segments with a height approximately twice the width. For this shape the efficiency advantage over the circular tube was nearly 3%. However, since non-circular tubes are likely to be somewhat more expensive to manufacture than circular tubes, it is an open question as to whether non-circular tubes are optimal from an economic standpoint.

## **Acknowledgements**

This work performed under the auspices of the U.S. Department of Energy by  
Livermore National Laboratory under Contract DE-AC52-07NA27344.

## Nomenclature

A	A representative point of reflection from the concentrator mirror
C	A point at the bottom of the concentrator mirror in the x-y plane
D	Width of parabolic concentrator mirror aperture
F	The focal point in the x-y plane for the parabolic trough mirror
FWHM	The full width at half maximum of a distribution
LS-3	Luz System Three Parabolic Trough Collector
SEGS	Solar Electric Generation System
d	diameter of circular heat collection element
f	focal length of parabolic concentrator mirror
h	the height of rhombic heat collection element in the y direction
r	distance from point of reflection A to mirror focus F in x-y plane
w	the width of a rhombic heat collection element in the x direction
x-y plane	the plane perpendicular to the longitudinal axis of symmetry of the parabolic trough
x	horizontal coordinate in the x-y plane
y	vertical coordinate in the x-y plane
$\alpha$	product of solar reflectivity and concentrator absorbance
$\beta$	angle between the y-axis and reflected sunlight ray direction
$\omega$	Apparent angular width of the heat collection element as seen from a given point of reflection from the parabolic concentrator mirror

## Optimal Heat Collection Element Shapes for Parabolic Trough Concentrators

- $\sigma^2$  variance of the angular spread of reflected sun-rays in the x-y plane
- $\sigma_{\parallel}^2$  variance of the mirror slope errors producing deviations of the local surface normal vector parallel to the parabolic trough axis
- $\sigma_{\perp}^2$  variance of the mirror slope errors producing deviations of the local surface normal vector perpendicular to the parabolic trough axis
- $\theta_{\parallel}$  Angle between the incident solar rays and the x-y plane

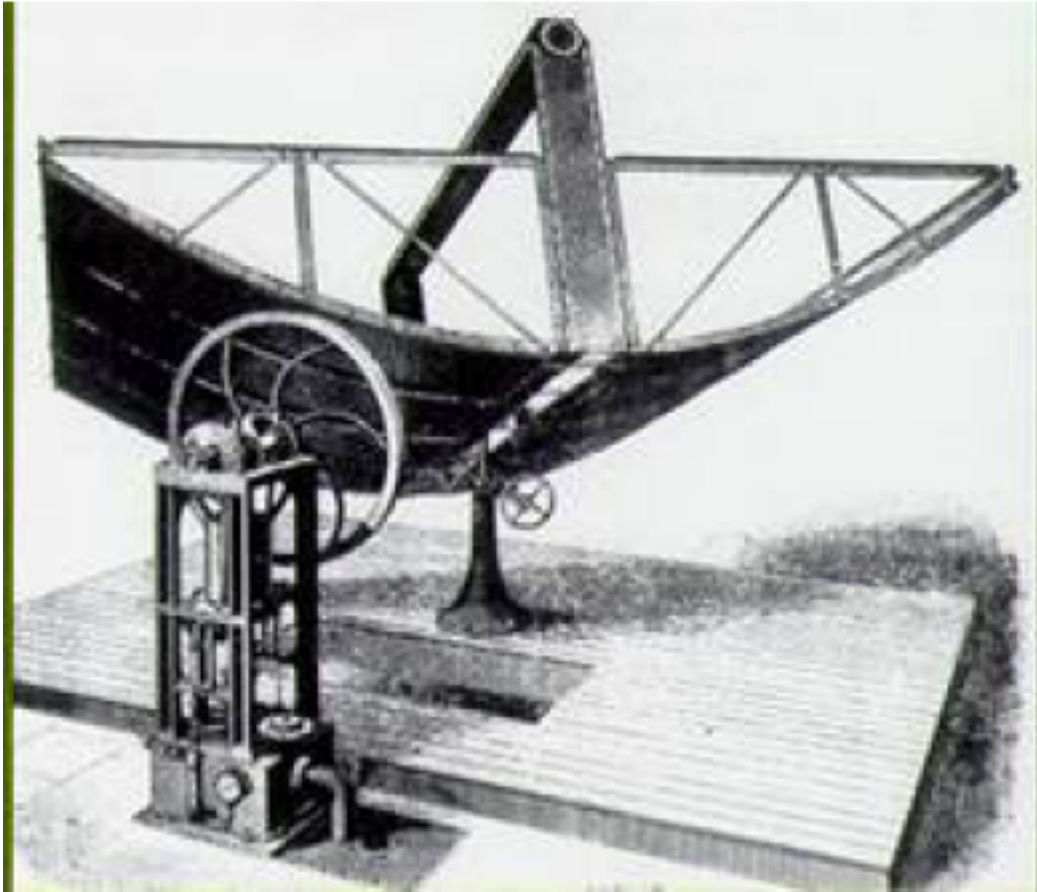


Fig. 1. A drawing of the parabolic trough solar concentrating mirror and hot air engine built by John Ericsson in 1883 is shown. Ericsson's "Sun-motor" was a form of Stirling engine. The heat collection tube at the focus is clearly circular. It is also notable that Ericsson's trough was not horizontal, and indeed featured a universal joint so that the mirror could be positioned to directly face the sun.

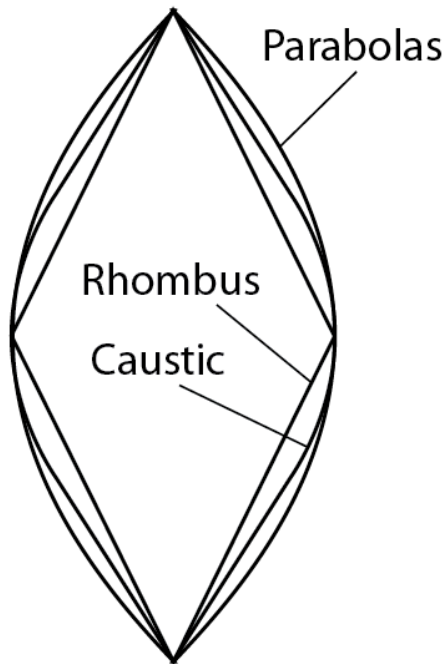


Fig. 2. The shapes of three types of heat collection element profiles are displayed. Each shape has a height to width ratio of 2. The shape labeled “Caustic” is a minimal absorber according to the recipe of Ries and Spirkl for a parabolic concentrating mirror having  $f/D=0.25$ . The shape labeled “Parabolos” corresponds to segments from a pair of parabolic curves having a common focus at the center of the figures, and is Cobble’s optimal shape. The third shape is a simple Rhombus, having a height twice its width.

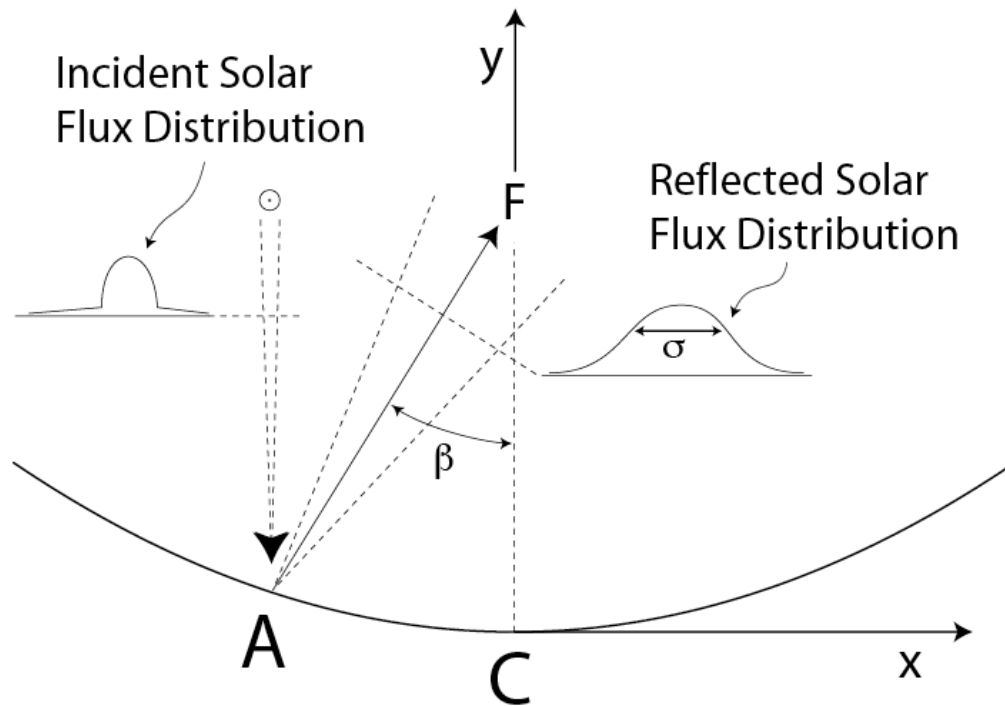


Fig. 3. An illustration of the effects of surface slope errors on the distribution of reflected sun light is displayed in the x-y plane perpendicular to the parabolic trough longitudinal symmetry axis.

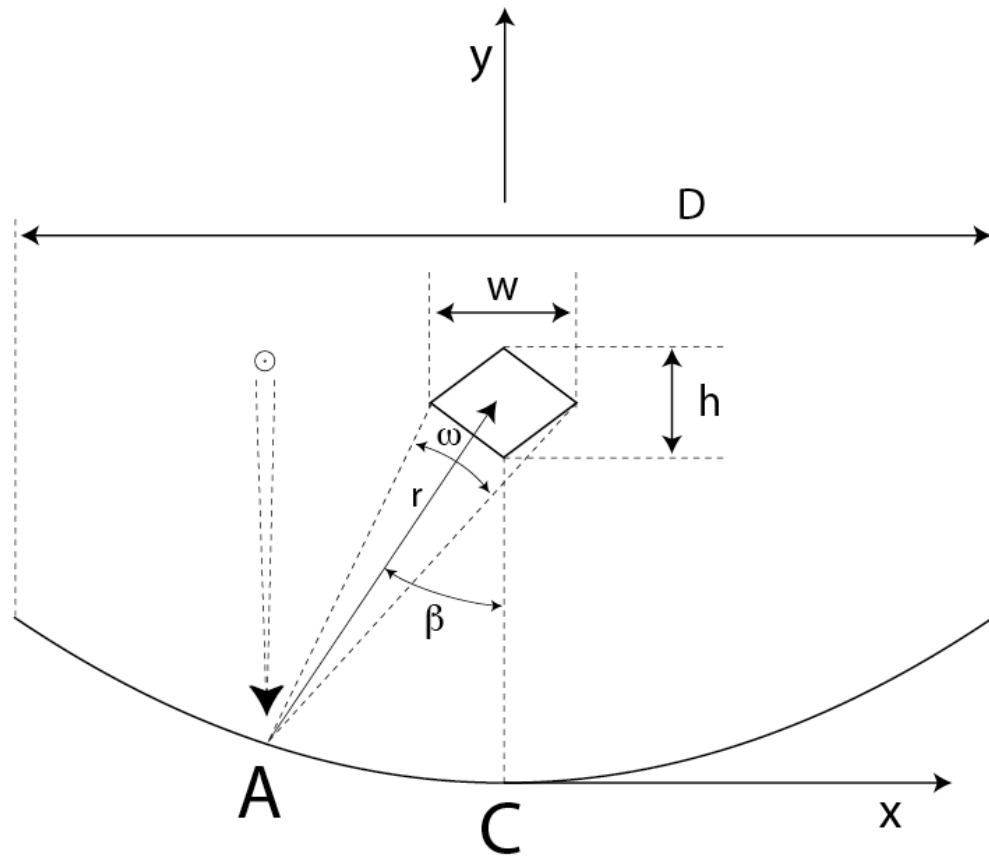


Fig. 4. An illustration of the case of a rhombus shaped heat collection element is shown.

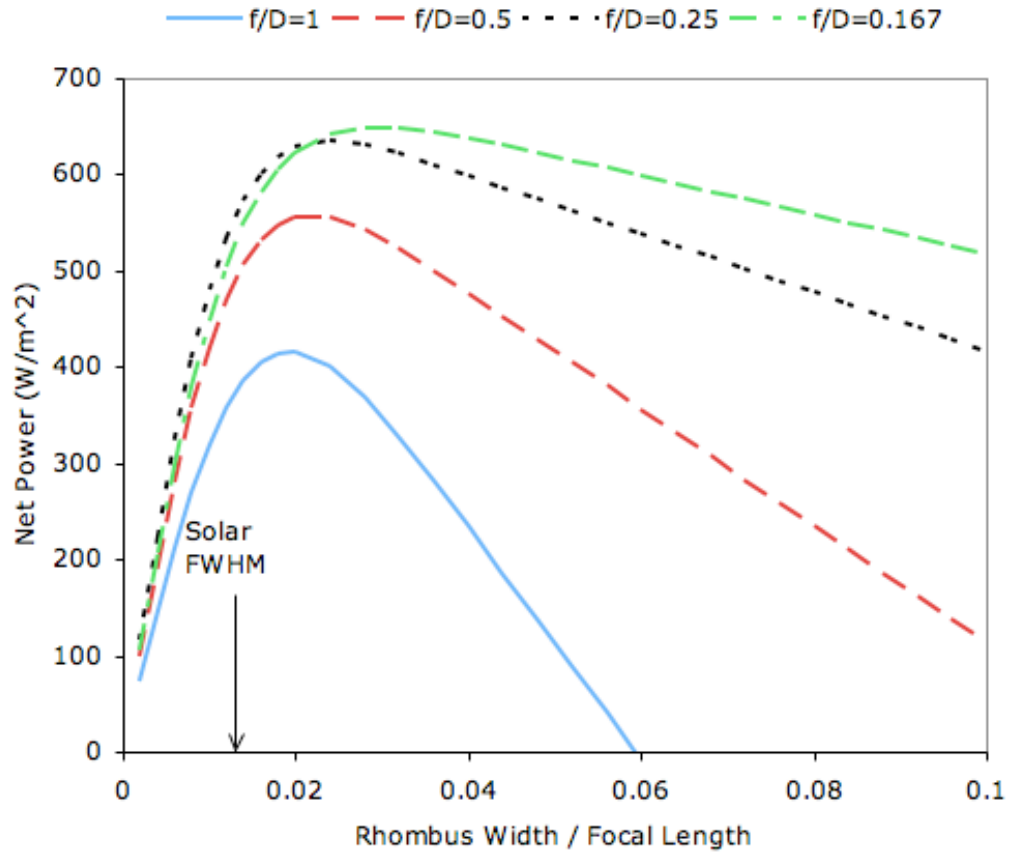


Fig. 5. Curves of the net thermal power collected are shown as a function of the width of a rhombic heat collection element for various focal length to aperture diameter  $f/D$  ratios. The arrow indicates the value of the FWHM for the reflected solar flux Gaussian distribution assumed.

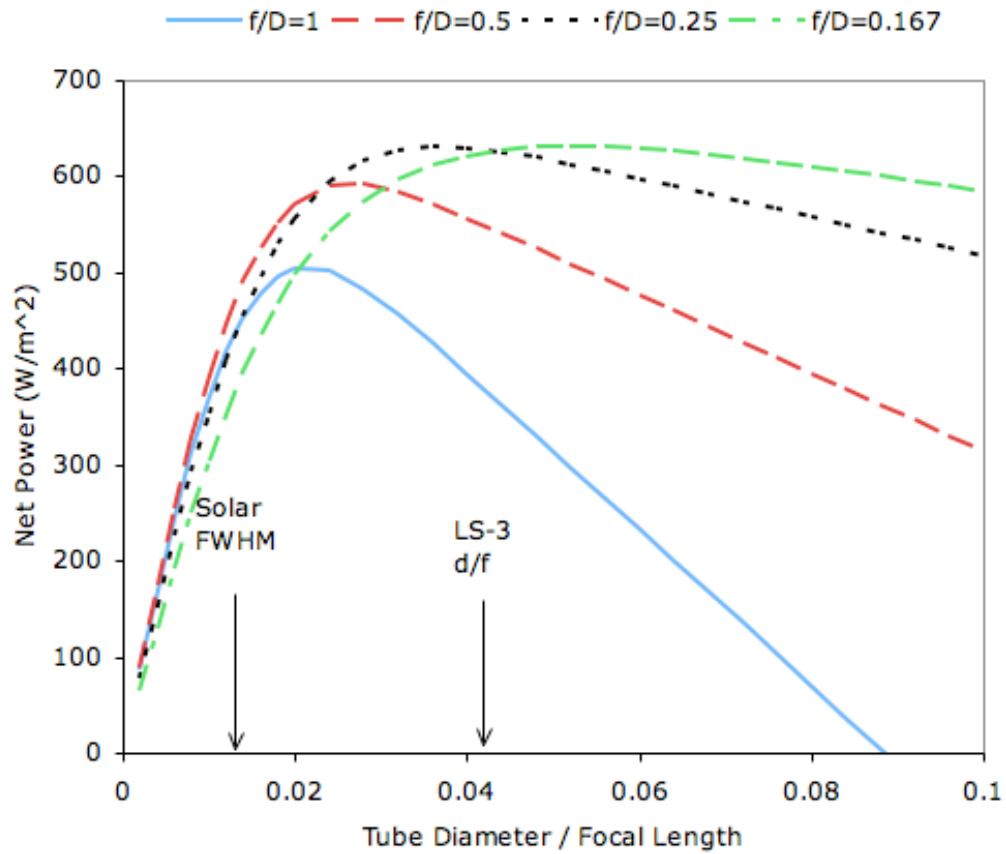


Fig. 6. Curves of the net thermal power collected are shown as a function of the diameter of a circular heat collection element for various focal length to aperture diameter  $f/D$  ratios. The right hand arrow indicates the absorbing tube diameter to focal length for the LS-3 heat collection elements used in the SEGS plants. The  $f/D$  ratio equals 0.288 for the SEGS mirrors.

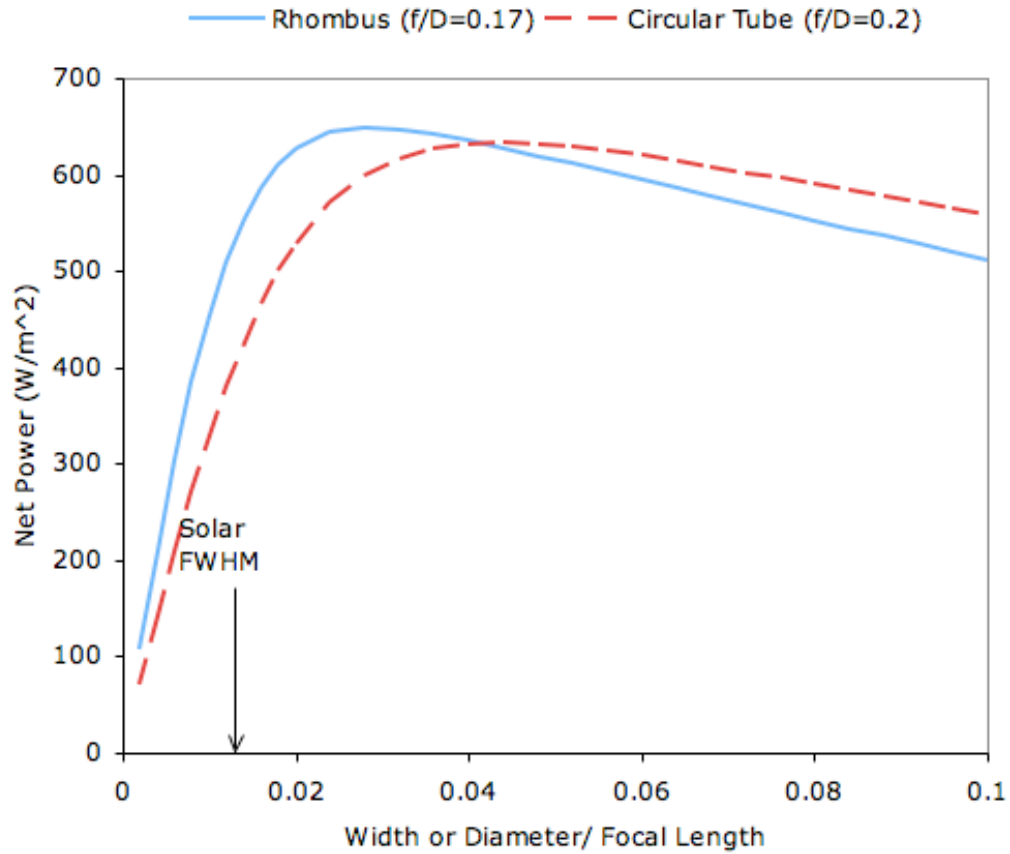


Fig. 7. A curve of the net thermal power collected for the rhombic collector with a concentrating mirror having  $f/D=0.17$  is compared with the curve for the circular tube collector with a concentrating mirror having  $f/D=0.20$ . The height to width ratio is 2.12 for the rhombic collector.

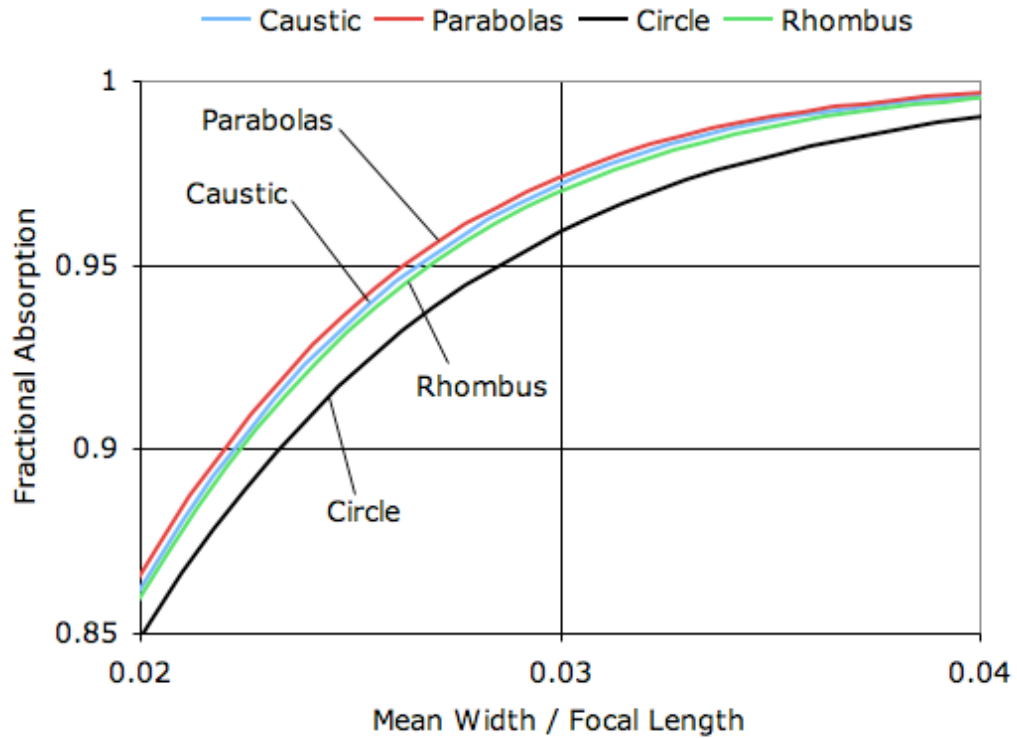


Fig. 8. The fractional absorption as a function of the mean width to focal length ratio is displayed for four different choices for the shape of the profile of the heat collection element. These curves, non-intersecting over the displayed range, are explicitly labeled in the figure. In this case, the reflected sunlight distribution is assumed to have a normal distribution with an r.m.s. angular width of 5.3 mrad.

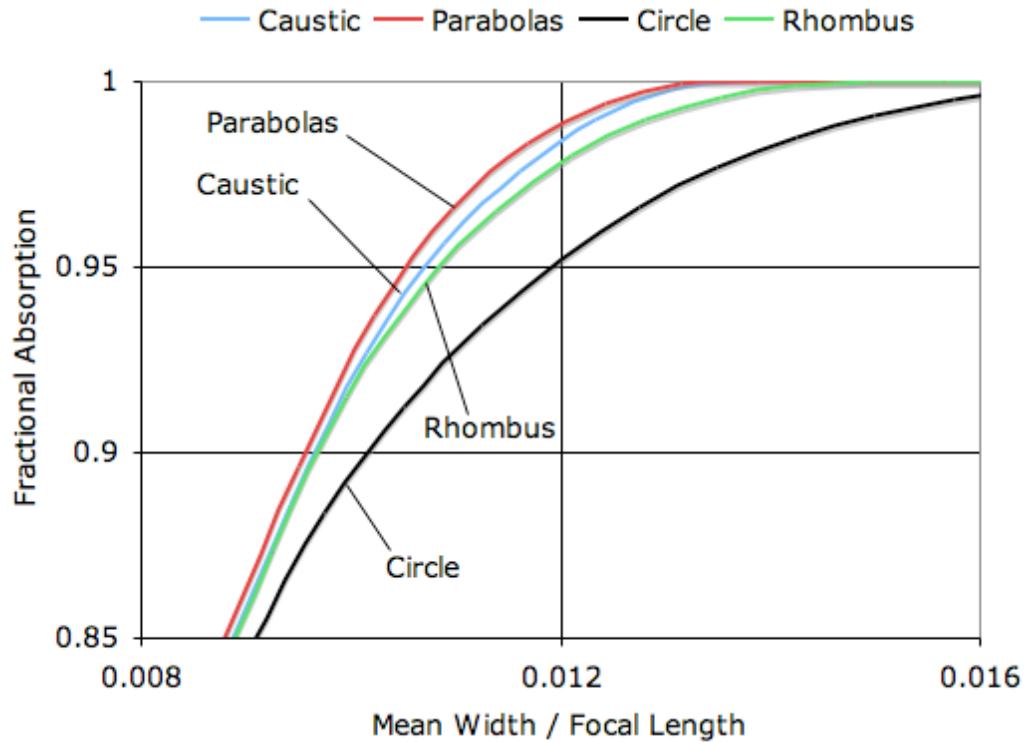


Fig. 9. The fractional absorption as a function of the mean width to focal length ratio is displayed for four different choices for the shape of the profile of the heat collection element. These curves, non-intersecting over the displayed range, are explicitly labeled in the figure. In this case, the solar angular distribution is assumed to be completely unaffected by optical aberrations or atmospheric scattering.

## References

---

- [1] William Conant Church, *The Life of John Ericsson, Vol. II*, (Charles Scribner's sons, New York, 1890), p265.
- [2] William Conant Church, *The Life of John Ericsson, Vol. II*, (Charles Scribner's sons, New York, 1890), p269.
- [3] H. Price, "Concentrating Solar Power Systems Analysis and Implications", slide 39, available at [http://www1.eere.energy.gov/solar/pdfs/3solar\\_henryprice.pdf](http://www1.eere.energy.gov/solar/pdfs/3solar_henryprice.pdf)
- [4] H. Ries and W. Spirkel, "Caustic and its use in designing optimal absorber shapes for 2D concentrators", in Nonimaging Optics: Maximum Efficiency Light Transfer III, Roland Winston, ed., SPIE proceedings, Vol. 2538 (1995), p. 2-9
- [5] M.H. Cobble, "Theoretical concentrations for solar furnaces", *Solar Energy*, Vol. 5, (1961) pp. 61-72.
- [6] T. Wendelin, "Parabolic Trough VSHOT Optical Characterization in 2005-2006", presented at the 2006 Parabolic Trough Technology Workshop in Incline Village, NV, available from the website: [www.eere.energy.gov/troughnet/2006\\_parabolic\\_trough\\_tech\\_workshop.html](http://www.eere.energy.gov/troughnet/2006_parabolic_trough_tech_workshop.html)
- [7] P. Bendt, A. Rabi, H.W. Gaul, K.A. Reed, "Optical Analysis and Optimization of Line Focus Solar Collectors", Solar Energy Research Institute report no. TR-34-092, (1979), especially see equation 2-18 on p. 11

